HPU2 Journal of Sciences:
Natural Sciences and Technology

journal homepage: https://sj.hpu2.edu.vn

Article type: Research article

Investigation of structural and electronic properties of ZnO using first principle calculations

Quoc-Van Duong*

Hanoi National University of Education, Hanoi, Vietnam

Abstract

In this research, first-principle calculations have been performed to study the geometry structure and electronic properties of ZnO. All possible exchange-correlation energy functionals were used to perform geometry optimization of ZnO in order to find the efficient calculation conditions. Bandgap energy, density of states (DOS), projected DOS (PDOS); and other properties of ZnO were also calculated and discussed. The calculated band-gap value of ZnO is less than 1.0 eV, much smaller than experimental value of 3.37 eV; while the PDOS results indicate the important roles of O 2p and Zn 3d orbitals in ZnO band structures. The well-known limitation of band-gap value calculations using Density Functional Theory (DFT) was solved by applying Hubbard potential on Zn 3d and O 2p orbitals. A full investigation with Hubbard value varying from 0.5 to 10 eV has been performed and the selected value is 8.0 eV for both Zn 3d and O 2p electrons.

Keywords: ZnO, DFT, pseudopotential, Hubbard potential, electronic structure

1. Introduction

ZnO is an attractive semiconductor due to its interesting physical properties: wide and direct band-gap value (3.37 eV), high electron mobility and high thermal conductivity [1], [2]. ZnO has been used in many products such as medicine, cosmetics, food, rubber and solar cells [3]. In photocatalytic application, ZnO has shown the high efficiency on photodegradation of different organic compounds like methyl orange [4] or methylene blue [5], [6]. The photocatalytic activity of ZnO can be affected by various parameters like purity, particle sizes and shapes [7], [8] or light absorbance ability. The wide band-gap value and high electron-hole recombination rate can also decrease the efficiency of

* Corresponding author, E-mail: vandq@hnue.edu.vn

https://doi.org/10.56764/hpu2.jos.2024.3.1.78-87

Received date: 25-9-2023 ; Revised date: 27-02-2024 ; Accepted date: 13-3-2024

photocatalytic process of ZnO [9]. The two common ways to improve ZnO photocatalytic activity are doping with other elements or compositing it with other materials. A variety of elements have been doped into ZnO for this purpose such as Fe [10], Co [11], Ni [12], Al or Ga [13], Ti or V [14]. ZnO is also composited, with other materials such as CNTs [15], Fe_3O_4 [16] or perovskite like $SrTiO_3$ [17]. The results show that the photocatalytic activity of ZnO has been improved, suggesting that these solutions are applicable for real life application. This improvement can be predicted by first-principle calculations in order to guide the sample fabrication process, which has been done by both free or commercial software packages like SIESTA [18], VASP [19], [20], WIEN2k [21], [22], Quantum ESPRESSO [23], CASTEP [24]–[29] and more [30].

ZnO lattice constants can be achieved using geometry optimization, which has been performed using various software packages and codes based on Density Functional Theory (DFT), but the calculation conditions are not coincident. Two possible approximation for exchange-correlation were investigated along with different parameterizations. Using CASTEP, Adnan et al. [29] suggested that Local Density Approximation (LDA) with Perdew-Zunger parameterization (PZ) should be used for calculating properties of ZnO, consistent with results of Alharshan et al. [31] and other studies [32]–[34]. On the other hand, Haffad et al. [18] used SIESTA to show that Generalized Gradient Approximation (GGA) parameterized with Perdew-Burke-Ernzerhof (PBE) functional gives the best calculated lattice parameter of ZnO, agreed with experimental result [1] and calculations [24], [27], [35] while Hamzah et al. [25] indicate that PBESol is a better option when calculating with CASTEP. Recently, Arfaoui et al. [36] proved that both GGA-PBE and GGA-PBESol can be used for calculating the structural, electronic and optical properties of ZnO in the framework of Quantum ESPRESSO while Ali [28] uses CASTEP to indicate that Wu-Cohen (WC) parametrization exhibit better results for same purpose.

For electronic properties calculation, the well-known limitation of DFT is that the calculated band-gap energy of ZnO is smaller than the expected value, which is consequence of ignoring the electron-electron interactions in the materials [37]. To overcome this limitation, Hubbard potential can be applied to valence electrons, Zn 3d and O 2p for the case of ZnO. Hamzah et al. [25] show that the acceptable Hubbard potentials for Zn and O are U_d = 5 and U_p = 9 eV, respectively. Harun et al. [33] prove that Hubbard potentials U_d = 5 eV and U_p = 7 eV need to be applied to 3d- and 2p-state electrons of ZnO to achieve a bandgap value of 3.10 eV using Materials Studio while the corresponding values of U_d = 10.57 eV and U_p = 7.1 eV were presented by Qiao et al. [38]. When using ABINIT, Goh et al. [30] show that there are 2 possible pairs of Hubbard potentials - U_d = 9.5 eV and U_p = 7.86 eV or U_d = 10.0 eV and U_p = 7.74 eV - can be used depending on the other calculate parameters. Thang et al. [20] show that a Hubbard value of 4.7 eV can be used for Zn 3d electrons when calculated with VASP.

The obtained results show a conflict in the determination of calculation conditions, leading to a confusion for researchers to select. In this research, a complete investigation on the effects of pseudopotentials and Hubbard values on the properties of this material has been done using Materials Studio software. The obtained parameters can be used for latter calculation in order to explain and predict the physical properties of ZnO-based materials.

2. Experimental Methods

The calculations were performed using Cambridge Serial Total Energy (CASTEP) [1], [2] - a first principle program based on density functional theory (DFT) to calculate the properties for a wide range of materials such as alloys, compounds, ceramics, semiconductors, metals and more, which was embedded in Materials Studio [3] - a commercial software used for material science. Both Local Density Approximation (LDA) and Generalized Gradient Approximation (GGA) were used for the exchange-correlation functional with the different parametrizations: Perdew-Zunger (CA-PZ) [4], Perdew-Burke-Ernzerhof (PBE) [5], Revised PBE (RPBE) [6] and Perdew-Wang (PW91) [7].

The calculations were executed on a pure ZnO unit cell, containing 2 Zn atoms and 2 O atoms, as shown in Figure 1. The Monkhorst-Pack scheme k-point grid sampling [8] was sets at 2×2×1 in the supercell. The interactions between the core and valence electrons ($3d^{10}4s^2$ for Zn and $2s^22p^4$ for O) are described by Vanderbilt ultrasoft pseudopotential [9]. The Hubbard potentials [10], representing for electron-electron interactions, were both applied to 3d-state electrons of Zn and 2p-state of O with the values in the range of 0 to 10 eV. The energy change, maximum force, maximum stress and maximum displacement tolerances in the geometry optimization processes were set at 5×10^{-6} eV/atom, 0.01 eV/Å, 0.02 GPa and 0.005 Å, respectively.

3. Results and discussion

3.1. Structural Properties

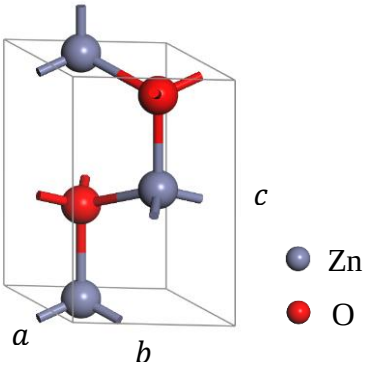

Figure 1. Unit cell of ZnO.

Table 1. Optimized structures of ZnO.

Functional	a = b (Å)	c (Å)
LDA-PZ	3.1861	5.1497
GGA-PBE	3.2841	5.2960
GGA-RPBE	3.3146	5.3463
GGA-PW91	3.2896	5.2913
Calculated [11]	3.2340	5.2720
Experiment [12]	3.2490	5.2040
JCPDS 36-1451	3.2498	5.2066

Table 1 shows the lattice constants of ZnO calculated using Materials Studio with different functionals, previous work and experiment. All optimized structures have hexagonal lattice system where a = b ≠ c and α = β = 90°, γ = 120°. It can be seen that GGA-PBE gives the best results in geometry optimization with the lattice constants of a = 3.2841 Å and c = 5.2960 Å, in good agreement with experimental values [12] and previous theoretical works [13]–[15].

Figure 2 shows the band structures of ZnO calculated using different functionals: LDA-PZ, GGA-PBE, GGA-RPBE and GGA-PW91. All obtained results show that ZnO is a direct band-gap semiconductor, the smallest band-gap value originated at G-G transition, in good agreement with previous studies [11], [16]. The values of band-gap calculated using LDA, PBE, RPBE and PW91 are 1.076 eV, 0.800 eV, 0.824 eV and 0.793 eV, respectively. These values are larger than the calculated

results of Mohamad et al. [16] or Haffad et al. [11], close to the work of Hassan [17] but much smaller than the experimental value 3.37 eV [12]. The deviation in band-gap values is the consequence of ignoring interaction between valence electron in the material, similar to the calculated band-gap for TiO_2 [18], is the consequence of well-known limitations related to the basis of DFT [19]. This deviation can be solved by adding Hubbard potential [10] to the corresponding valence electrons – 3d and 4s for Zn and 2p for O in the case of ZnO.

3.2. Electronic Structures

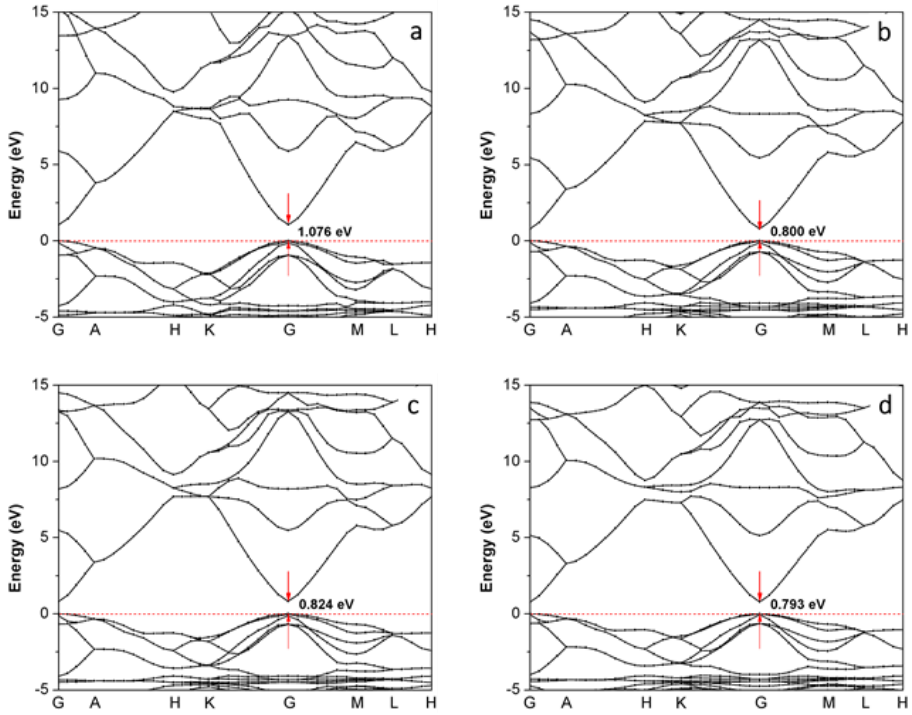

Figure 2. Band structures of ZnO calculated using (a) LDA-PZ, (b) GGA-PBE, (c) GGA-RPBE and (d) GGA-PW91.

Figure 3 presents the density of states (DOS) of ZnO calculated using GGA-PBE in the range of -10 eV to 15 eV. Both valence bands, from -0 eV to 0 eV, and conduction band, from 1 eV to 15 eV result almost from the hybridization of Zn 3d and O 2p orbitals, consistent with previous calculations [16], [20]. The projected density of states of Zn and O in Figure 3b and 3c also indicates that Zn 4s electrons contribute an insignificant part in the formation of ZnO band structure from -10 eV to 15 eV, details can be seen in the work of Bakhtiar et al. [21]. The negligible contribution of Zn 4s suggest that Hubbard potential can be considered for Zn 3d and O 2p valence electrons only.

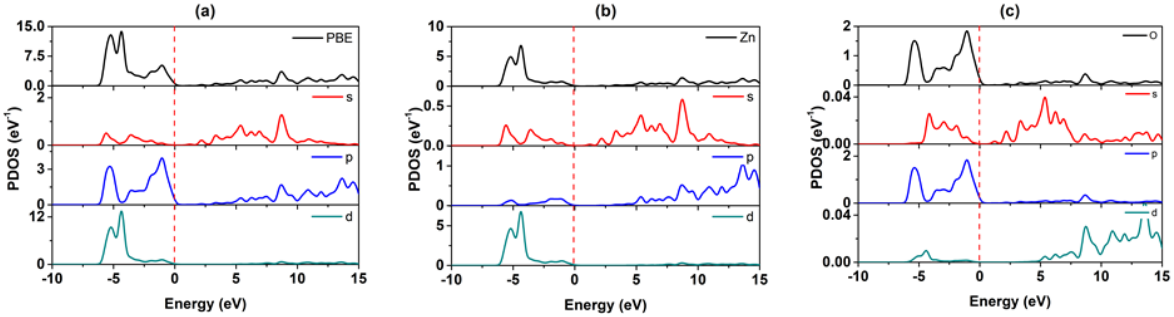

Figure 3. Partial Density of State (PDOS) of (a) ZnO, (b) Zn and (c) O in ZnO.

3.3. Zn-O bondings

The electron deformation density of ZnO can be calculated $\boldsymbol{\Delta\rho(r) = \rho_{ZnO} - \rho_{Zn} - \rho_{O}}$ whereas $\boldsymbol{\rho_{ZnO}}$ is the electron density of ZnO, $\boldsymbol{\rho_{Zn}}$ and $\boldsymbol{\rho_{O}}$ are the electron densities of Zn atoms and O atoms only [36]. Figure 4 shows the electron deformation density of a ZnO unit cell calculated using GGA-PBE at the isosurface of ±0.05. The red color indicates the accumulation while the blue color represents the depletion of electron in the region. In ZnO, the electron density of Zn decreases while the electron density of O decreases, suggests that valence electrons have transferred from Zn to O to form the covalence bonds, in good agreement with experiment [37].

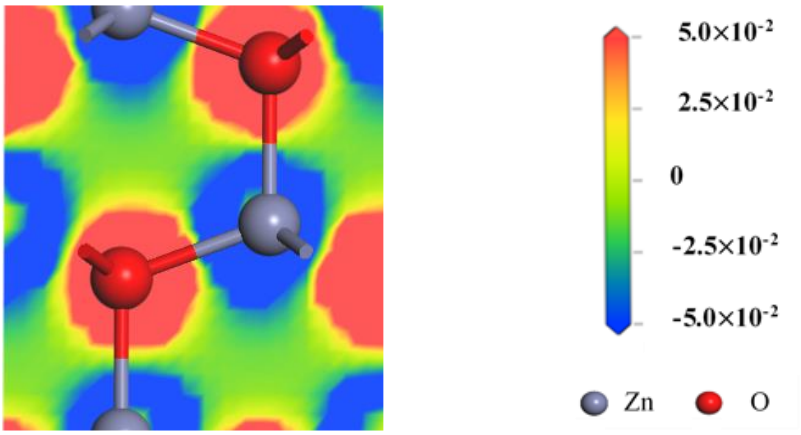

Figure 4. Electron deformation density of ZnO.

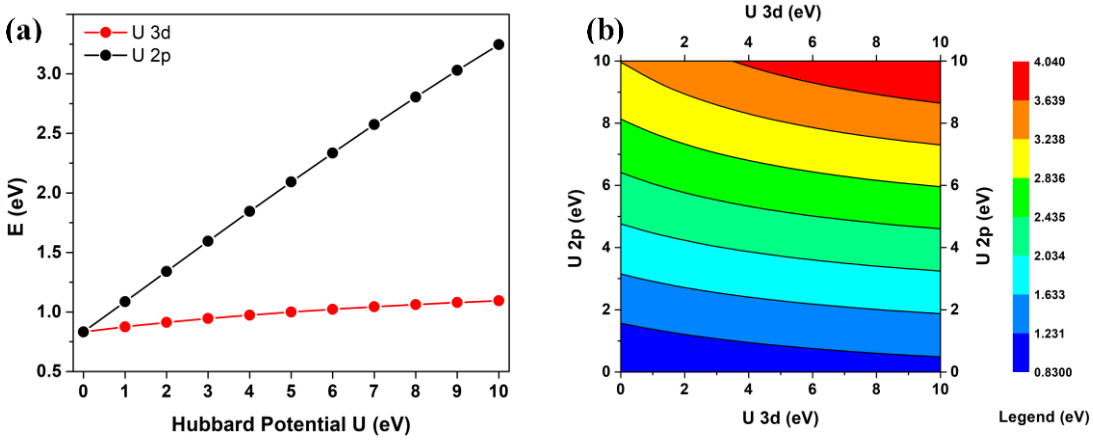

Figure 5. (a) The calculated of band-gap values of ZnO using Hubbard for Zn 3d or O 2p orbitals and (b) the contour of Hubbard potentials on ZnO.

3.4. A DFT+U Investigation of ZnO

The GGA-PBE functional gives the best results in geometry optimization but the calculated band-gap value is 0.80 eV, much smaller than the experimental value of 3.37 eV [12]. This drawback is the consequence of ignoring the valence electron-electron interactions in materials - a well-known limit of density functional theory. The two most common methods to solve this problem are using scissors operator [1], [2] or Hubbard potential [10]. In this research, different values of Hubbard potential were applied to Zn 3d (denoted as U 3d) and O 2p (denoted as U 2p) electrons of ZnO to investigate the change of band-gap energies.

Figure 5a shows the change of ZnO band-gap energies when the Hubbard potentials U were applied only on Zn 3d (U 3d) or O 2p (U 2p) orbitals. The Hubbard potential has more effects on O 2p electrons than on Zn 3d electrons, which can be seen on the tangents of the two graphs. The band-gap of ZnO only shows a significant change when the value of U 3d applied on Zn 3d electron reach 7.0 eV, is consistent with previous studies [30], [33]. To estimate the effects of Hubbard potential on both Zn 3d and O 2p valence electrons, all possible pairs of U 3d and U 2p from 0 eV to 10 eV with step of 0.5 eV have been used. The pairs of U 3d and U 2p and the corresponding calculated band-gap values were illustrated on Figure 5b. It can be seen that when the U 2p reaches 8.0 eV, the U 3d can be adjusted to obtained the band-gap around 3.2 eV to 3.6 eV, including the experimental value of 3.37 eV. This result is s with previous results of Qiao [38] and Goh [30].

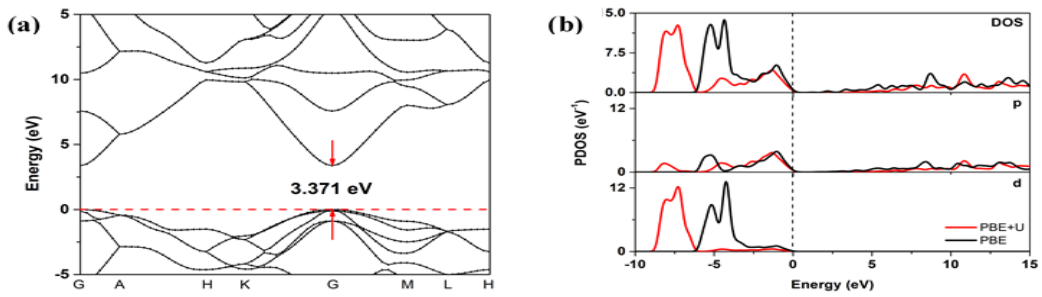

Figure 6. (a) The band structure and (b) projected density of states of ZnO calculated using GGA-PBE+U with Hubbard parameter U = 8.0 eV for both Zn 3d and O 2p orbitals.

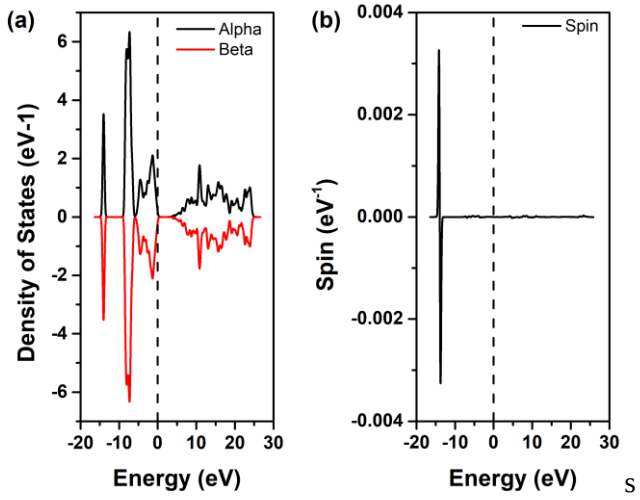

Figure 7. Total density of states of ZnO and spin-up and spin-down distribution.

For more details, electronic structures of ZnO with Hubbard potentials for both Zn 3d and O 2p electrons should be calculated and discussed. Figure 3 and its analysis suggest that the contribution of Zn 3d and O 2p in the formation of ZnO band structure are nearly equal, so are the values of U 3d and U 2p. In the latter calculation, the chosen values of both U 3d and U 2p are 8.0 eV. Figure 6a shows that the calculated band-gap value of ZnO with this pair of Hubbard potential is 3.371 eV, in good agreement with experimental result [12]. The density of states of ZnO calculated using GGA-PBE and GGA-PBE+U in Figure 6b shows significant changes in the valence and conduction bands of ZnO due to the effect of Hubbard potential. The stronger interactions between Zn 3d and O 2p electrons reduce the widths of valence and conduction bands, shift the lowest unoccupied molecular orbital in conduction bands of ZnO to the higher energy levels and reduce the band-gap of ZnO, consistent with the finding of Qiao et al. [22].

Table 2. Integrated Spin Densities of ZnO.

Material	**Integrated Spin Density** $\left(\frac{\hbar}{2}\right)$	**Integrated |Spin Density|** $\left(\frac{\hbar}{2}\right)$	**Magnetic Behavior**
ZnO	0.38×10^{-14}	0.53×10^{-4}	Ferromagnetic

To estimate the magnetic properties of intrinsic ZnO, the distribution of spin-up (alpha) and spin-down (beta) electrons and the total spin density of states were calculated using PBE+U and displayed on Figure 7. It can be seen that the density of states corresponds to spin-up and spin-down electrons are equal, as shown in Figure 7a, suggests that ZnO is a non-magnetic material, in good agreement with previous studies [21]. However, the calculated integrated spin densities of ZnO in Table 2 suggests that intrinsic ZnO exhibits weak ferromagnetic behavior [39], consistent with non-zero spin density of state on Figure 7a. Figure 8 shows the isosurfaces of spin density of ZnO – the yellow isosurface represents the spin density of 3.75×10^{-6} e/Å^3 whiles the blue one represents for the negative values. This result suggests that the ferromagnetic behavior of ZnO may originate from O atoms.

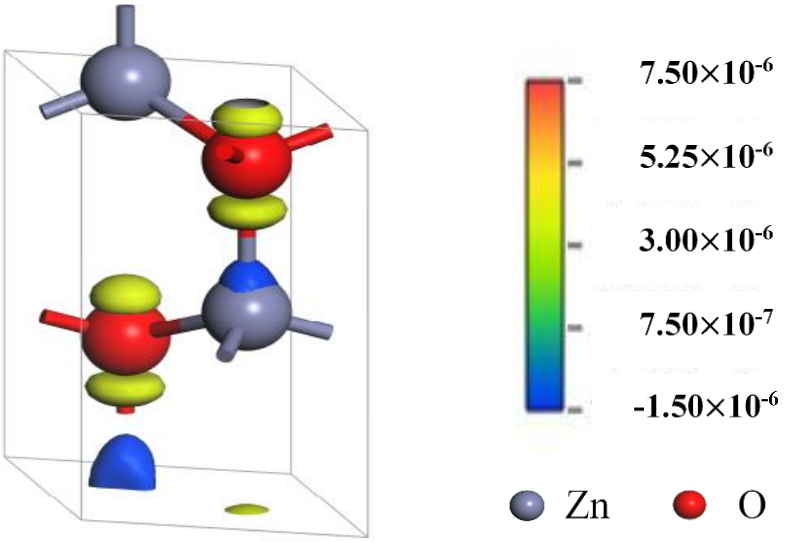

Figure 8. The isosurfaces of spin densisty of states of ZnO.

4. Conclusion

Structural and electronic properties of ZnO have been calculated using CASTEP computer code with different approximation and functionals. All calculations show that ZnO is a direct band-gap semiconductor, the minimum band-gap appears around G-G transition. The GGA-PBE gives the best result in geometry optimization and was chosen for later calculations. The calculated band-gap energy using GGA-PBE is much smaller than experimental value, while the PDOS result shows that the valence and conduction bands originated from hybridization of Zn 3d and O 2p electrons. The electron deformation density of ZnO shows that the Zn-O is a covalence bond. A complete investigation on the effect of Hubbard potential on 3d and 2p electrons has been done, and a pair of U 3d and U 2p of 8.0 and 8.0 eV has been chosen. The obtained band-gap with Hubbard potential applied to 3d and 2p electrons is 3.371 eV, in good agreement with experimental value. The further investigation on integrated spin density of states suggests that intrinsic ZnO exhibits weak ferromagnetic behavior, which may have originated from O atoms.

References

[1] Ü. Özgür *et al*., "A comprehensive review of ZnO materials and devices," *J. Appl. Phys.*, vol. 98, no. 4, p. 041301, Aug. 2005, doi: 10.1063/1.1992666.

[2] A. Janotti and C. G. Van de Walle, "Fundamentals of zinc oxide as a semiconductor," *Reports Prog. Phys.*, vol. 72, no. 12, p. 126501, Oct. 2009, doi: 10.1088/0034-4885/72/12/126501.

[3] C. Klingshirn, "ZnO: Material, physics and applications," *ChemPhysChem*, vol. 8, no. 6, pp. 782–803, Apr. 2007, doi: 10.1002/cphc.200700002.

[4] S. Bhatia and N. Verma, "Photocatalytic activity of ZnO nanoparticles with optimization of defects," *Mater. Res. Bull.*, vol. 95, no. 6, pp. 468–476, Nov. 2017, doi: 10.1016/j.materresbull.2017.08.019.

[5] J. R. Torres-Hernández *et al.*, "Structural, optical and photocatalytic properties of ZnO nanoparticles modified with Cu," *Mater. Sci. Semicond. Process.*, vol. 37, no. 6, pp. 87–92, Sep. 2015, doi: 10.1016/j.mssp.2015.02.009.

[6] K. Yu, J. Shi, Z. Zhang, Y. Liang, and W. Liu, "Synthesis, characterization, and photocatalysis of ZnO and Er-doped ZnO," *J. Nanomater.*, vol. 2013, pp. 1–5, Sep. 201, doi: 10.1155/2013/372951.

[7] Z. L. Wang, "Zinc oxide nanostructures: growth, properties and applications," *J. Phys. Condens. Matter*, vol. 16, no. 25, pp. R829–R858, Jun. 2004, doi: 10.1088/0953-8984/16/25/r01.

[8] T. Vu Anh, T. A. T. Pham, V. H. Mac, and T. H. Nguyen, "Facile controlling of the physical properties of zinc oxide and its application to enhanced photocatalysis," *J. Anal. Methods Chem.*, vol. 2021, no. 25, pp. 1–12, Apr. 2021, doi: 10.1155/2021/5533734.

[9] F. Zhang *et al.*, "Recent advances and applications of semiconductor photocatalytic technology," *Appl. Sci.*, vol. 9, no. 12, p. 2489, Jun. 2019, doi: 10.3390/app9122489.

[10] R. Elilarassi and G. Chandrasekaran, "Optical, electrical and ferromagnetic studies of ZnO:Fe diluted magnetic semiconductor nanoparticles for spintronic applications," *Spectrochim. Acta Part A Mol. Biomol. Spectrosc.*, vol. 186, no. 12, pp. 120–131, Nov. 2017, doi: 10.1016/j.saa.2017.05.065.

[11] J. Wojnarowicz, T. Chudoba, S. Gierlotka, K. Sobczak, and W. Lojkowski, "Size control of cobalt-doped ZnO nanoparticles obtained in microwave solvothermal synthesis," *Crystals*, vol. 8, no. 4, p. 179, Apr. 2018, doi: 10.3390/cryst8040179.

[12] S. Kunj and K. Sreenivas, "Defect mediated ferromagnetism in cluster free Zn 1−x Ni x O nanopowders prepared by combustion method," *J. Ind. Eng. Chem.*, vol. 60, no. 4, pp. 151–159, Apr. 2018, doi: 10.1016/j.jiec.2017.10.051.

[13] M. Khuili, G. El Hallani, N. Fazouan, H. A. El Makarim, and E. H. Atmani, "First-principles calculation of (Al,Ga) co-doped ZnO," *Comput. Condens. Matter*, vol. 21, no. 4, p. e00426, Dec. 2019, doi: 10.1016/j.cocom.2019.e00426.

[14] B. Ul Haq, R. Ahmed, A. Shaari, R. Hussain, and M. binti Mohamad, "DFT Investigations of Ti, V doped ZnO based diluted magnetic semiconductors," *Adv. Mater. Res.*, vol. 1107, pp. 502–507, Jun. 2015, doi: 10.4028/www.scientific.net/amr.1107.502.

[15] A. Kołodziejczak-Radzimska and T. Jesionowski, "Zinc oxide-from synthesis to application: A review," *Materials*, vol. 7, no. 4, pp. 2833–2881, Apr. 2014, doi: 10.3390/ma7042833.

[16] O. Długosz, K. Szostak, M. Krupiński, and M. Banach, "Synthesis of Fe3O4/ZnO nanoparticles and their application for the photodegradation of anionic and cationic dyes," *Int. J. Environ. Sci. Technol.*, vol. 18, no. 3, pp. 561–574, Jul. 2020, doi: 10.1007/s13762-020-02852-4.

[17] Y. Wu, B. Dong, J. Zhang, H. Song, and C. Yan, "The synthesis of ZnO/SrTiO3 composite for high-efficiency photocatalytic hydrogen and electricity conversion," *Int. J. Hydrogen Energy*, vol. 43, no. 28, pp. 12627–12636, Jul. 2018, doi: 10.1016/j.ijhydene.2018.03.206.

[18] S. Haffad, G. Cicero, and M. Samah, "Structural and electronic properties of ZnO nanowires: A theoretical study," *Energy Procedia*, vol. 10, pp. 128–137, Jul. 2011, doi: 10.1016/j.egypro.2011.10.165.

[19] X. H. Zhou, Q.-H. Hu, and Y. Fu, "First-principles LDA+U studies of the In-doped ZnO transparent conductive oxide," *J. Appl. Phys.*, vol. 104, no. 6, p. 063703, Sep. 2008, doi: 10.1063/1.2978324.

[20] H. V. Thang, D. V. T. Tram, P. L. M. Thong, D. T. Quang, and P. C. Nam, "B and Au doped ZnO and ZnO/Cu(111) bilayer films: A DFT investigation," *Vietnam J. Chem.*, vol. 60, no. 3, pp. 323–332, Jun. 202224, doi: 10.1002/vjch.202100125.

[21] B. Ul Haq, R. Ahmed, A. Shaari, and S. Goumri-Said, "GGA+U investigations of impurity d-electrons effects on the electronic and magnetic properties of ZnO," *J. Magn. Magn. Mater.*, vol. 362, pp. 104–109, Aug. 2014, doi: 10.1016/j.jmmm.2014.03.033.

[22] B. U. Haq, A. Afaq, R. Ahmed, and S. Naseem, "Structural, electronic, and magnetic properties of Co-doped ZnO," *Chinese Phys. B*, vol. 21, no. 9, p. 097101, Sep. 2012, doi: 10.1088/1674-1056/21/9/097101.

[23] A. Apaolaza, D. Richard, and M. Tejerina, "Experimental and ab initio study of the structural and optical properties of ZnO coatings: Performance of the DFT+U approach," *Process. Appl. Ceram.*, vol. 14, no. 4, pp. 362–371, Otc. 2020, doi: 10.2298/pac2004362a.

[24] H. Soleimani, "CASTEP study on electronic and optical properties of zinc oxid," *Recent Adv. Petrochemical Sci.*, vol. 1, no. 3, May 2017, doi: 10.19080/rapsci.2017.01.555563.

[25] N. Hamzah *et al.*, "A DFT+U study of structural, electronic and optical properties of Ag- and Cu-doped ZnO," *Microelectron. Int.*, vol. 40, no. 1, pp. 53–62, Jan. 2023, doi: 10.1108/mi-05-2022-0088.

[26] J. Gulomov, O. Accouche, R. Aliev, R. Ghandour, and I. Gulomova, "Investigation of n-ZnO/p-Si and n-TiO2 /p-Si Heterojunction Solar Cells: TCAD + DFT," *IEEE Access*, vol. 11, pp. 38970–38981, Jan. 2023, doi: 10.1109/access.2023.3268033.

[27] M. Basseem, A. A. Emam, F. H. Kamal, A. M. Gamal, and S. A. Abo Faraha, "Novel functionalized of ZnO with Sm3+, La3+, and Sr2+/ZnO single and tri-doped nanomaterials for photocatalytic degradation:

synthesis, DFT, kinetics," *J. Mater. Sci.*, vol. 58, no. 33, pp. 13346–13372, Aug. 2023, doi: 10.1007/s10853-023-08829-1.

[28] A. Ali, "Hubbard model calculations for zinc oxide semiconductor," *Univ. Thi-Qar J. Sci.*, vol. 10, no. 1, pp. 101–106, Jun. 2023, doi: 10.32792/utq/utjsci/v10i1.988.

[29] M. Adnan *et al.*, "DFT Investigation of the structural, electronic, and optical properties of AsTi (Bi)-phase ZnO under pressure for optoelectronic applications," *Materials*, vol. 16, no. 21, p. 6981, Oct. 2023, doi: 10.3390/ma16216981.

[30] E. S. Goh, J. W. Mah, and T. L. Yoon, "Effects of Hubbard term correction on the structural parameters and electronic properties of wurtzite ZnO," *Comput. Mater. Sci.*, vol. 138, pp. 111–116, Oct. 2017, doi: 10.1016/j.commatsci.2017.06.032.

[31] G. A. Alharshan *et al.*, "Optical band gap tuning, DFT understandings, and photocatalysis performance of ZnO nanoparticle-doped Fe compounds," *Materials*, vol. 16, no. 7, p. 2676, Mar. 2023, doi: 10.3390/ma16072676.

[32] A. A. Mohamad *et al.*, "First-principles calculation on electronic properties of zinc oxide by zinc–air system," *J. King Saud Univ.-Eng. Sci.*, vol. 29, no. 3, pp. 278–283, Jul. 2017, doi: 10.1016/j.jksues.2015.08.002.

[33] K. Harun, N. Mansor, Z. A. Ahmad, and A. A. Mohamad, "Electronic properties of ZnO nanoparticles synthesized by sol-gel method: A LDA+U calculation and experimental study," *Procedia Chem.*, vol. 19, pp. 125–132, Jan. 2016, doi: 10.1016/j.proche.2016.03.125.

[34] A. Janotti and C. G. Van de Walle, "LDA + U and hybrid functional calculations for defects in ZnO, SnO2 , and TiO2," *Phys. status solidi*, vol. 248, no. 4, pp. 799–804, Apr. 2011, doi: 10.1002/pssb.201046384.

[35] M. Mohammadzaheri, S. Jamehbozorgi, M. D. Ganji, M. Rezvani, and Z. Javanshir, "Toward functionalization of ZnO nanotubes and monolayers with 5-aminolevulinic acid drugs as possible nanocarriers for drug delivery: A DFT based molecular dynamic simulation," *Phys. Chem. Chem. Phys.*, vol. 25, no. 32, pp. 21492–21508, Jan. 2023, doi: 10.1039/d3cp01490h.

[36] Y. El Arfaoui, M. Khenfouch, and N. Habiballah, "DFT and SCAPS-1D calculations of FASnI 3 -based perovskite solar cell using ZnO as an electron transport layer," *Eur. Phys. J. Appl. Phys.*, vol. 98, p. 60, Oct. 2023, doi: 10.1051/epjap/2023230099.

[37] N. E. Kirchner-Hall, W. Zhao, Y. Xiong, I. Timrov, and I. Dabo, "Extensive benchmarking of DFT+U calculations for predicting band gaps," *Appl. Sci.*, vol. 11, no. 5, p. 2395, Mar. 2021, doi: 10.3390/app11052395.

[38] L. Qiao, C. Chai, Y. Yang, X. Yu, and C. Shi, "Strain effects on band structure of wurtzite ZnO: a GGA + U study," *J. Semicond.*, vol. 35, no. 7, p. 073004, Jul. 2014, doi: 10.1088/1674-4926/35/7/073004.

[39] J. Goldsby, S. Raj, S. Guruswamy, and D. D. Azbill, "First-Principle and Experimental Study of a Gadolinium-Praseodymium-Cobalt Pseudobinary Intermetallic Compound," *J. Mater.*, vol. 2015, p. 753612, Jun. 2015, doi: 10.1155/2015/753612.